JUSTC

Article

http://justc.ustc.edu.cn

Received: September 27, 2022; Accepted: October 04, 2023

Infrared microthermometry of fluid inclusion in sphalerite: A case study of the Xinqiao deposit in the Middle–Lower Yangtze metallogenic belt

Yangyang Wang[1], and Yilin Xiao[1,2] ✉

[1]*CAS Key Laboratory of Crust-Mantle Materials and Environments, School of Earth and Space Sciences, University of Science of Technology of China, Hefei 230026, China;*
[2]*CAS Center for Excellence in Comparative Planetology, Hefei 230026, China*

✉Correspondence: Yilin Xiao, E-mail: ylxiao@ustc.edu.cn

Graphical abstract

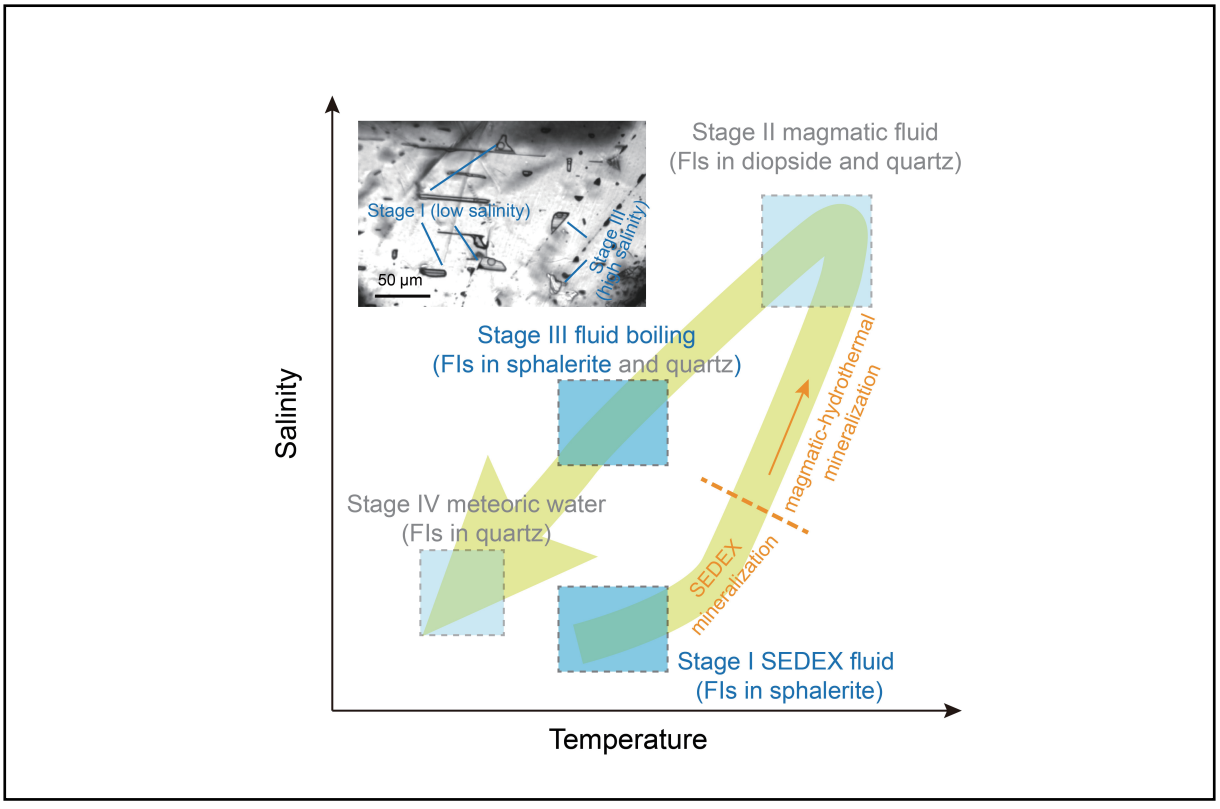

Fluid inclusions (FIs) in sphalerite and other minerals recorded a four-stage ore-forming fluid evolution in the Xinqiao deposit.

Public summary

- Low light intensity can minimize temperature deviations during infrared microthermometry.
- Sphalerite-hosted fluid inclusions in the Xinqiao deposit are aqueous and have two groups with contrasting salinity.
- The Xinqiao deposit is formed by two-stage metallogenic events including sedimentary exhalative and magmatic-hydrothermal mineralization.

Citation: Wang Y Y, Xiao Y L. Infrared microthermometry of fluid inclusion in sphalerite: A case study of the Xinqiao deposit in the Middle–Lower Yangtze metallogenic belt. *JUSTC*, **2024**, 54(5): 0502. DOI: 10.52396/JUSTC-2023-0054

JUSTC

Article

http://justc.ustc.edu.cn

Received: September 27, 2022; Accepted: October 04, 2023

Infrared microthermometry of fluid inclusion in sphalerite: A case study of the Xinqiao deposit in the Middle–Lower Yangtze metallogenic belt

Yangyang Wang[1], and Yilin Xiao[1,2] ✉

[1]*CAS Key Laboratory of Crust-Mantle Materials and Environments, School of Earth and Space Sciences, University of Science of Technology of China, Hefei 230026, China;*
[2]*CAS Center for Excellence in Comparative Planetology, Hefei 230026, China*

✉Correspondence: Yilin Xiao, E-mail: ylxiao@ustc.edu.cn

Cite This: *JUSTC*, **2024**, 54(5): 0502 (12pp) Read Online SI Supporting Information

Abstract: Infrared microthermometry allows direct measurement of fluid inclusions hosted in opaque ore minerals and can provide direct constraints on the evolution of ore-forming fluids. This study presents infrared microthermometry of sphalerite-hosted fluid inclusions from the Xinqiao deposit in the Middle-Lower Yangtze Metallogenic Belt and sheds new light on the ore genesis of the deposit. Considering that infrared light may lead to non-negligible temperature deviations during microthermometry, some tests were first conducted to ensure the accuracy of the microthermometric measurements. The measurement results indicated that using the lowest light intensity of the microscope and inserting an optical filter were effective in minimizing the possible temperature deviations of infrared microthermometry. All sphalerite-hosted fluid inclusions from the Xinqiao deposit were aqueous. They show homogenization temperature ranging from ~200 to 350 °C, but have two separate salinity groups (1.0%–10% and 15.1%–19.2% NaCl equivalent). The low-salinity group represents sedimentary exhalative (SEDEX)-associated fluids, whereas the high-salinity group results from modification by later magmatic hydrothermal fluids. Combined with published fluid inclusion data, the four-stage fluid evolution of the Xinqiao deposit was depicted. Furthermore, our data suggest that the Xinqiao deposit was formed by two-stage metallogenic events including SEDEX and magmatic-hydrothermal mineralization.

Keywords: Infrared microthermometry; fluid inclusion; sphalerite; the Xinqiao deposit

CLC number: P618.43 **Document code:** A

1 Introduction

Fluid inclusion studies can provide a unique perspective for deciphering complex geological processes, particularly for, constraining ore-forming fluid evolution and precipitation mechanisms of ore-forming materials for a given ore deposit. Because of the opaque signature of most ore minerals under visible light, previous studies have generally been conducted on transparent gangue minerals (such as quartz), with the inference that gangue minerals were co-precipitated with ore minerals from the same fluid. This inference is generally based on field observation, which means that the relationship between gangue and ore minerals is doubtful in many cases. Even intimately intergrown mineral pairs have frequently been shown to precipitate from different fluids or at different stages[1–10]. Fortunately, a few ore minerals that are opaque under visible light are transparent to translucent under infrared light. Therefore, infrared light microscopy allows direct observation of opaque ore minerals and the direct microthermometry of the fluid inclusions hosted by them[1,2,7,10,11–18].

The middle-lower Yangtze River region is one of the most important metallogenic belts in China and has developed a series of middle-large porphyry-, skarn-, and porphyrite-type polymetallic deposits. Although numerous studies have demonstrated intimate relationships between mineralization and Yanshanian magmatism (~120–150 Ma)[19–21], the ore genesis of these deposits remains highly debated. Among these deposits, the Xinqiao Cu-Au-Fe-S deposit in the Tongling district represents a typical polymetallic deposit involving a complex and probably multi-stage ore-forming process. Two metallogenic events have been proposed: (1) skarn-type mineralization associated with Yanshanian magmatism and (2) marine volcanic exhalation during the Paleozoic[22–28]. Both metallogenic events have been verified by sulfide Re-Os dating which generally shows two separate isochron ages (~319–393 Ma and ~138 Ma)[23,25]. Previous fluid inclusion studies have also been conducted, but mainly on gangue minerals such as quartz and diopside[25,29]. In particular, Wang et al. [25] revealed that fluid boiling and fluid mixing between magmatic fluid and meteoric water played a significant role in the Yanshanian metallogenic event. Similarly, Li et al.[29] depicted a continuous fluid evolution associated with skarn formation and proposed an Early Cretaceous carbonate replacement origin for the Xinqiao deposit. It should be noted that both studies assumed that the gangue minerals and ore

DOI: 10.52396/JUSTC-2023-0054
JUSTC, **2024**, 54(5): 0502

minerals (mainly sulfides) precipitated from the same fluid [25, 29]. Direct studies of fluid inclusions hosted in sulfides are thus required to validate this assumption to help build a comprehensive metallogenic model of the Xinqiao deposit.

By employing infrared microthermometry, we conducted fluid inclusion studies on spherite from the Xinqiao deposit to provide direct constraints on ore-forming fluids and to help improve our understanding of this type of deposit. Beforehand, we provide a simple review of infrared microthermometry to elaborate on its principles and on some key technical issues when applied to natural samples.

2 An overview of infrared microthermometry

2.1 Background to infrared microthermometry

The transmittance of a mineral depends on its band structure and light energy. Many minerals (particularly ore minerals) are classified as semiconductors. According to band theory, there is a band gap between the valence and conduction bands of a semiconductor. The gap represents the minimum energy for exciting an electron to move from valence band to conduction band[30]. Each mineral has a unique band gap[31]. As visible light energy is around 1.7–3.3 eV, any minerals (such as quartz or carbonate) having band gap energies higher than 1.7 eV will not absorb all the visible light and thus be transparent or semi-transparent. In contrast, minerals with a band gap energy lower than 1.7 eV absorb all visible light and are thus opaque, which is the case for the majority of ore minerals.

Infrared light has a longer wavelength (0.73 to 1000 μm), and thus lower photon energy (0.00124 to 1.7 eV) than visible light. Consequently, when minerals have band gap energies lower than 1.7 eV, they allow at least some infrared light to pass through, i.e., they are transparent or semi-transparent under infrared light. For example, chalcopyrite has a band gap energy of ~1.1 eV[30], which means it absorbs all light with wavelengths less than 1130 nm but light can pass through it at higher wavelengths.

Infrared microscopy provides an opportunity to conduct petrological observations of opaque minerals. This can be realized after a few modifications to a traditional microscope, for example, by mounting an infrared light source and an infrared light-specific objective lens. In addition, because infrared light cannot be observed with the naked eye, a specific piece of equipment must be mounted on the microscope to capture the image. Commercially available equipment includes a tube camera (such as the Hamamatsu tube camera) and a digital camera (such as an indium gallium arsenide camera, also called an InGaAs camera). They are both sensitive to different wavelength ranges, but are restricted to near-infrared light (730 to 2500 nm)[14]. Owing to this limitation, infrared microscopy is only applicable to minerals that near-infrared light can pass through. In theory, the observation of minerals with very low band gap energy requires a more advanced camera that is sensitive to mid and even far-infrared light. Nevertheless, direct fluid inclusion studies using a combination of infrared microscopy and a microthermometry stage or other in-situ analytical techniques have been conducted on various minerals, including pyrite, wolframite, stibnite, enargite, sphalerite, and rutile[7, 13–18, 32–34].

2.2 Warming effects of infrared radiation during microthermometry

The "warming" effects of infrared radiation may cause a significant deviation to the microthermometric results of fluid inclusion. Thus, possible temperature deviations between the microthermometric results obtained using infrared and visible light should be carefully inspected before applying infrared microthermometry to natural samples. It should be noted that there are some minor discrepancies between two commercial microthermometry stages (Linkam and United States Geological Survey, also called USGS) when measuring the same inclusion. By using a USGS stage, Lindaas et al. [35] found a standard deviation for a final melting temperature of ± 0.4 °C for five-time repeated measurements of the same inclusion. By contrast, a Linkam heating/freezing stage decreased the deviation to ± 0.1 °C. Many studies have reported limited temperature deviations when using the same stage but different light sources. For instance, after careful calibration of the thermocouples of the USGS stage by multiple measurements of synthetic fluid inclusion standards, Pflugbeil[36] reported consistent microthermometric results between visible and infrared light. This good consistency was further supported by subsequent studies on fluid inclusions in semi-transparent minerals (such as Fe-poor sphalerite) and some transparent minerals (such as quartz and fluorite) [1,2,11–13,37]. Even infrared microthermometry of fluid inclusions in some opaque minerals, such as pyrite and hematite, has had limited temperature deviations [38–41].

The temperature deviations, however, may be significant for many other minerals. Moritz[42] first reported significant temperature deviations during infrared microthermometry of fluid inclusions in enargite. The measured ice melting temperature (T_m) and homogenization temperature (T_h) decreased with increasing infrared light intensity. Subsequently, an increasing number of studies observed similar temperature deviations[43, 44]. Recently, Peng et al.[45] provided a thorough evaluation of temperature deviations during infrared microthermometry. They found that temperature deviations were mineral-dependent and closely related to light intensity. Finally, they proposed that the infrared light intensity should be as low as possible to minimize or using improved cycling methods to avoid the effects on microthermometry[45].

The host mineral must be transparent to infrared light during the entire microthermometry process to ensure complete temperature recording. However, the transmittance of minerals to infrared light decreases with increasing temperature. By employing Fourier transform infrared (FT-IR) spectroscopy, Lüders[14] found that the infrared light absorption edge of a wolframite crystal from Panasqueira, Portugal shifted to longer wavelengths with increasing temperature. Thus, the infrared light transmittance of wolframite decreases, considering the invariable detection wavelength range of the infrared camera[14]. This is similar to later observations of wolframite from San Cristobal[17]. The temperature dependence of transmittance has been reported for many minerals including

DOI: 10.52396/JUSTC-2023-0054
JUSTC, 2024, 54(5): 0502

stibnite, enargite, and pyrite[17]. Observable minerals become opaque when the temperature increases to a very high value, and the transition temperature depends on mineral composition and light wavelength[17]. Decreasing transmittance during the heating process may hinder the measurement of homogenization temperature, particularly when the host mineral becomes opaque before the fluid inclusion inside homogenizes.

2.3 Cycling microthermometry method

Considering the "warming" effects of infrared light radiation and the decreasing transparency of host minerals during microthermometry, a cycling microthermometry method was proposed by Goldstein and Reynolds[46] and then improved and widely used by Zhu et al. [47] and Peng et al. [45], to obtain accurate temperature records. This method takes full advantage of the undercooling signature (lower temperature than the phase transition temperature but with no phase changes) for the fluid phase and avoids infrared light irradiation during the heating process. For T_m measurements, changes in mineral transmittance are generally limited, and more attention should be paid to the thermal effects of infrared light radiation. The recommended measurement process includes four steps (Fig. 1a): 1) Freezing the inclusion by cooling to a very low temperature (T_1); 2) Turning off the infrared light and heating the inclusion to a temperature (T_3) that is slightly higher than the estimated eutectic temperature (T_2) of the inclusion system; 3) Cooling the inclusion to T_1 with the infrared light on and observing whether the bubble changes abruptly. There is generally no abrupt change in the bubble during this step; and 4) replacing T_3 at a slightly higher temperature T_4 and repeating Steps 2 and 3. The final temperature for heating during the repeat of Step 2 could be recorded as T_m once an abrupt change in the bubble is observed during cooling in the repeat of Step 3. Because temperature T_1 during the measurement is generally very low, which prolongs the measurement process, an alternative method can be used by modifying Step 3. Using the new method (Fig. 1b), the inclusion is cooled to temperature T_2 (estimated eutectic temperature for the inclusion system) in Step 3. During cooling, the bubble gradually changes if the frozen inclusion does not melt completely at Step 2. In contrast, T_m can be recorded when the bubble is first observed to remain unchanged during cooling in Step 3.

The above cycling method is also applicable for measuring T_h for a fluid inclusion, in which the final temperature during Step 3 cooling is set slightly lower than the estimated T_h and the key point for observation is whether there is a bubble in the inclusion (Fig. 2). The T_h is recorded when no bubble appears during the repeat of Step 3 cooling. Additionally, this method provides a possible way to measure inclusions that homogenize before the appearance of heating-induced opacity in their host mineral. Under these circumstances, the final temperature during Step 3 of cooling (T_2 in Fig. 2) can be

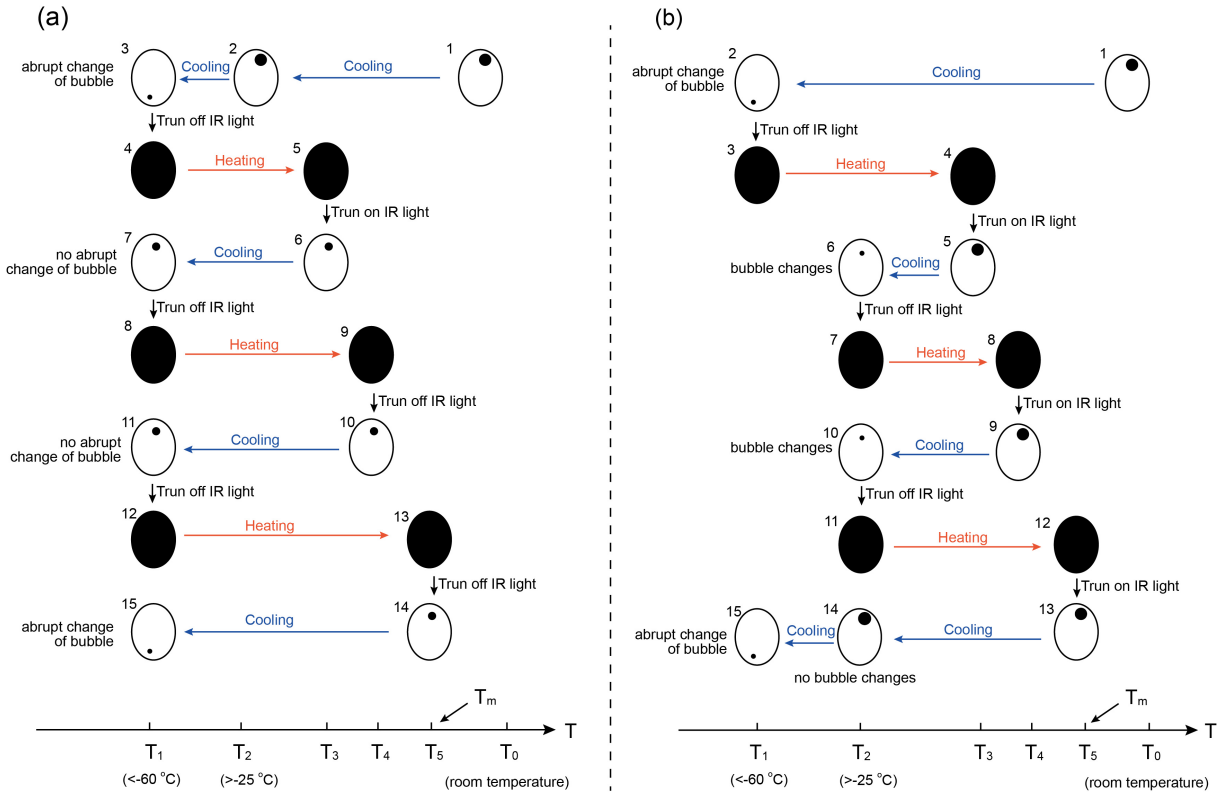

Fig. 1. Cycling method for infrared microthermometry to measure final ice melting temperature (T_m) of opaque minerals (modified after Goldstein and Reynolds [46] and Peng et al. [45]). T_0, T_1 and T_2 represent room temperature, a temperature low enough for freezing (generally < –60 °C) and estimated eutectic temperature of the target inclusion system. (a) The inclusion is cooled to T_1 to ensure freezing during every cooling step with infrared (IR) light on. During every heating step, the IR light is turned off and the final temperature for heating is set to be a little higher than the front heating step (T_5>T_4>T_3). The final temperature for heating is regarded as T_m once abrupt change of bubble is observed during the subsequent cooling step. (b) After the first cooling to freeze the inclusion, the final temperature for every cooling step is set to be around estimated eutectic temperature of the target inclusion system. T_m could be recorded when no bubble change is observed during the cooling step.

DOI: 10.52396/JUSTC-2023-0054
JUSTC, **2024**, 54(5): 0502

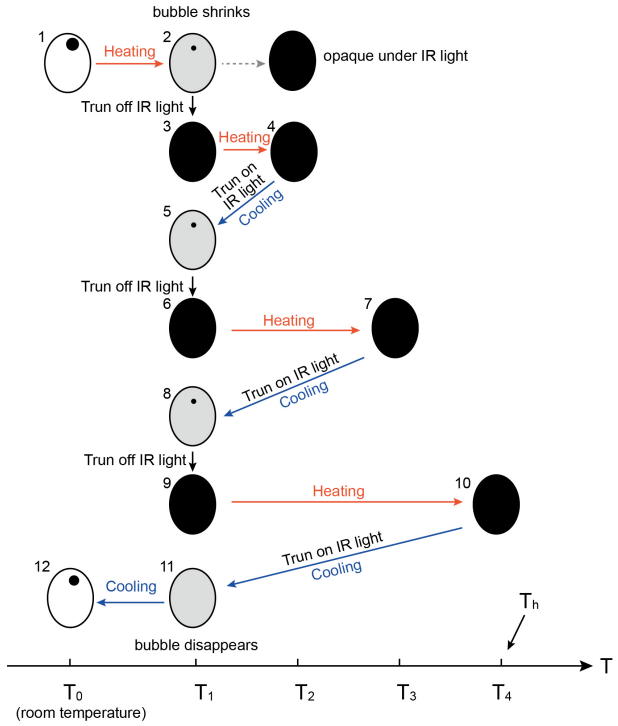

Fig. 2. Cycling method for infrared microthermometry to measure homogenization temperature (T_h) of opaque minerals (modified after Goldstein and Reynolds [46] and Peng et al. [45]). T_0 represents room temperature. T_1 is the temperature slightly lower than the estimated T_h or lower than the transition temperature for the host mineral to become opaque. For every heating step the infrared (IR) light is turned off and the final temperature is set to increase step by step. The IR light is turned on during the cooling steps in order to observe whether there is a bubble in the inclusion. The final temperature for heating during the cycles could be regarded as T_h when the bubble disappears after the subsequent cooling step.

set as the transition temperature at which the mineral becomes opaque (Fig. 2). However, the method is incapable of measuring the fluid inclusions that have T_h far higher than the "opacity-transition temperature" of their host mineral. On this occasion, the inclusions will consistently contain a bubble at "transition temperature" after cooling from any higher temperature, thus more advanced equipment (mid- and far-infrared light microscope) is required for further measurements.

The cycling microthermometry method has been successfully applied to various types of opaque ore minerals, contributing significantly to understanding the detailed evolution of ore-forming fluids[16, 48]. In many cases, infrared microthermometry studies of ore minerals have revealed a fluid evolution that is different from that recorded in gangue minerals, resulting in a significant improvement in the metallogenic mechanism[7, 18, 33].

3 Geological settings and sample description

The Xinqiao deposit is the largest Cu-Au-Fe-S polymetallic deposit in eastern China. The Jitou monzodiorite is the main magmatic rock related to mineralization in this region. It was dated at 140.4 ± 2.2 Ma by zircon SHRIMP U-Pb geochronology[49]. Among all the exposed strata from the Upper Devonian to the Lower Triassic in the region, the Upper Carboniferous dolostone and limestone are the dominant strata that are closely related to the ore body (Fig. 3). In addition to bedded sulfide along the strata, the skarn sulfide associated with the Jitou monzodiorite is the other type of ore body in the Xiaoqiao deposit but only accounts for ~10% of the gross reserves. The ore minerals of the deposit (including bedded and skarn ore bodies) include pyrite, chalcopyrite, pyrrhotite, magnetite, sphalerite and galena, and the gangue minerals comprise dolomite, calcite and quartz.

In this study, sphalerite from a bedded ore body was collected for infrared microthermometry. Sphalerite generally has an intergrowth relationship with pyrite and other sulfides, confirming the same genesis as that of the entire bedded ore body. The collected sphalerite was rufous or black in the hand specimens. Different colors, ranging from reddish-orange to black, were observed in different parts of the sphalerite crystals under a polarizing microscope. These probably suggest compositional variations (such as iron content) although the color variations were irregular. Overall, all sphalerites showed poor transmittance when visible light microscopy was used. Therefore, it was impractical to perform traditional microthermometric measurements. Using an infrared microscope, it was observed that the sphalerite contained abundant fluid inclusions (Fig. 3). The inclusions typically showed negative crystal or elliptical shapes and generally had two phases (liquid and vapor with no daughter minerals) with a bubble filling degree lower than 30% (Fig. 3). They were commonly isolated or gathered together as a fluid inclusion assemblage far from mineral boundaries or cracks. Based on the petrological criteria, these inclusions were classified as primary. It should be noted that some primary inclusions were dark, which may have been due to large differences in the refractive index at the inclusion boundary. In addition, a few small inclusions were distributed along the mineral boundaries and cracks, showing typical signatures of secondary origin.

4 Methods

With the cycling microthermometry method, microthermometric measurements of the primary inclusions were conducted at the University of Science and Technology of China, using a combined Olympus BX-53 infrared microscope and Linkam THMSG 600 heating/freezing stage with operating temperatures from −193 to 600 °C. The light intensity of the microscope was continuously adjusted from degree 1 (low) to degree 11 (high), whereas the field and condenser diaphragms were adjusted from fully open to fully closed, corresponding to values from 0.65 to 0 and from 1 to 0, respectively. A high-resolution infrared camera (sensitive to infrared light with a wavelength of 400–900 nm) and a medium-resolution infrared camera (sensitive to 900–1700 nm) were mounted on the microscope for image capture. The microthermometry stage was calibrated using synthetic fluid inclusions (USGS) with a visible light microscope. The precision was 0.2 °C and 1 °C for temperatures lower and higher than 31 °C, respectively. Prior to this, a synthetic CO_2 inclusion in quartz (from the USGS) and a saline inclusion in sphalerite from the Xinqiao deposit were selected for test measurements using the combined equipment to evaluate the possible

DOI: 10.52396/JUSTC-2023-0054
JUSTC, **2024**, 54(5): 0502

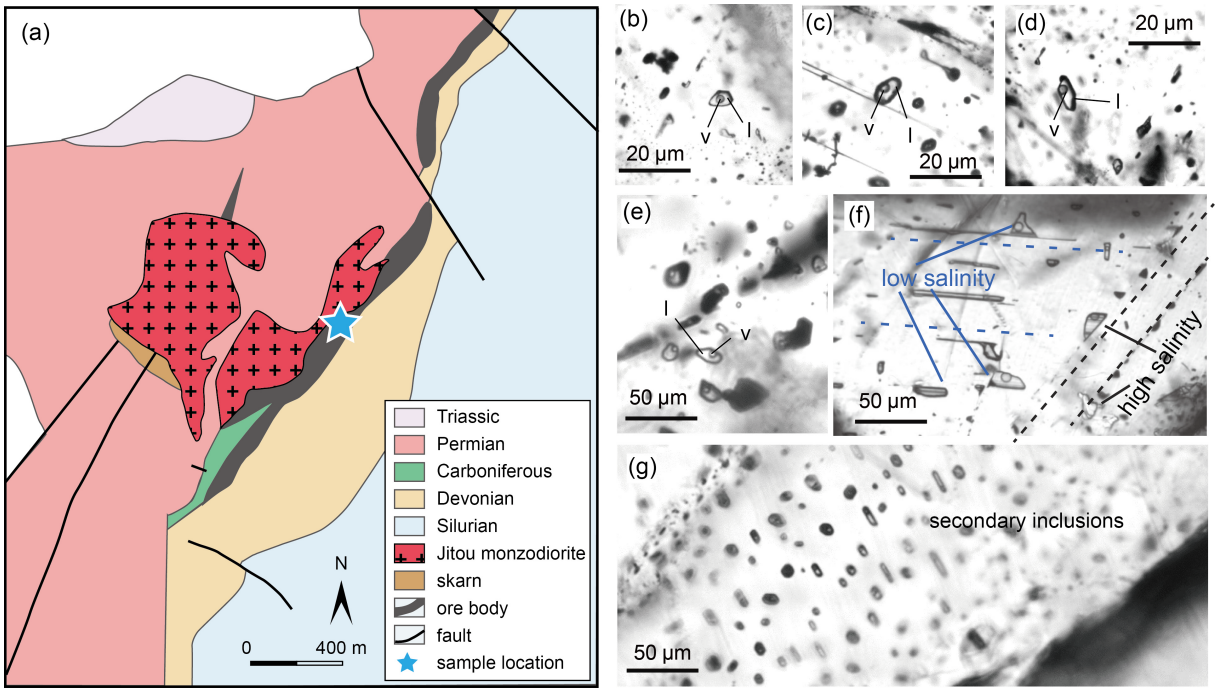

Fig. 3. Simplified geological map for the Xinqiao deposit (a) and fluid inclusions in sphalerite (b-g). The sample location is marked as blue star. All the fluid inclusions show primary signature except for the right bottom photo (g) in which the fluid inclusions are of secondary origin. (f) shows the relative age of different groups (low salinity versus high salinity) of fluid inclusions. l: liquid; v: vapor.

deviation of microthermometric data from different light intensities, field and condenser diaphragms. The microthermometry steps were as described by Wang et al. [25].

The test measurements demonstrated that low infrared light intensity, small field and condenser diaphragms, and the insertion of an optical filter could help reduce temperature deviations during microthermometry. The measurements of sphalerite-hosted fluid inclusions in the Xinqiao deposits followed optimized parameters that minimized any possible temperature deviations. Because the optical filter available in the laboratory (1200 nm) could only match the medium-resolution camera, an optical filter was not used for the majority of measurements. Moderate field and condenser diaphragms were used because very small diaphragms darkened the inclusion boundary in the digital image, making it difficult to observe the phase change of the fluid inclusions. Nevertheless, according to the test measurements, the lowest light intensity was sufficient to guarantee accurate results for most of the measurements. For some suitable inclusions (large in size and having thin boundary), repeated measurements were performed by reducing the diaphragms and inserting the 1200-nm optical filter. All of them showed temperature deviations that were much smaller than the measurement errors.

5 Results

5.1 Test measurements

Test measurements of quartz-hosted CO_2 inclusion and sphalerite-hosted saline inclusion showed different deviations for the measured T_m and T_h. The measured CO_2 melting and homogenization temperatures were identical to the recommended values when light with the lowest intensity was used (Fig. 4). However, the brightest light decreased the measured temperatures by 1.1 °C and 1.5 °C for CO_2 melting and homogenization temperatures, respectively (Fig. 4), which were much larger than the measurement errors. If light intensity is fixed, increasing the field or condenser diaphragms can decrease the measured temperature, similar to the effects of increasing light intensity. It should be noted that the measured temperatures were identical to the recommended values within error under a very small field or condenser diaphragms but under high infrared light intensity (degree 5–6 in the test measurements, Fig. 4b); this probably demonstrated the significant effects of the field and condenser diaphragms in decreasing the irradiation light intensity on the sample. After inserting the 1200-nm optical filter, the measured results were also identical to the recommended values even if the light intensity was very high and all the diaphragms were fully open.

The test measurements of sphalerite-hosted saline inclusions showed similar variation trends to those of quartz-hosted CO_2 inclusion. As there is no recommended value for the target inclusion, we took the value measured with the improved cycled method under conditions of the lowest light intensity, smallest field and condenser diaphragm, and inserting the 1200-nm optical filter as the reference value (Fig. 5). By changing light intensity, the deviations could be up to 10.2 °C and 12.8 °C for ice melting and homogenization temperatures, respectively (Fig. 5a). Similarly, decreasing the field and condenser diaphragms (with the same light intensity of 5) or inserting an optical filter could reduce or even eliminate the deviations (Fig. 5b).

5.2 Sphalerite-hosted fluid inclusion in the Xinqiao deposit

The eutectic temperatures of the studied inclusions ranged

DOI: 10.52396/JUSTC-2023-0054
JUSTC, **2024**, 54(5): 0502

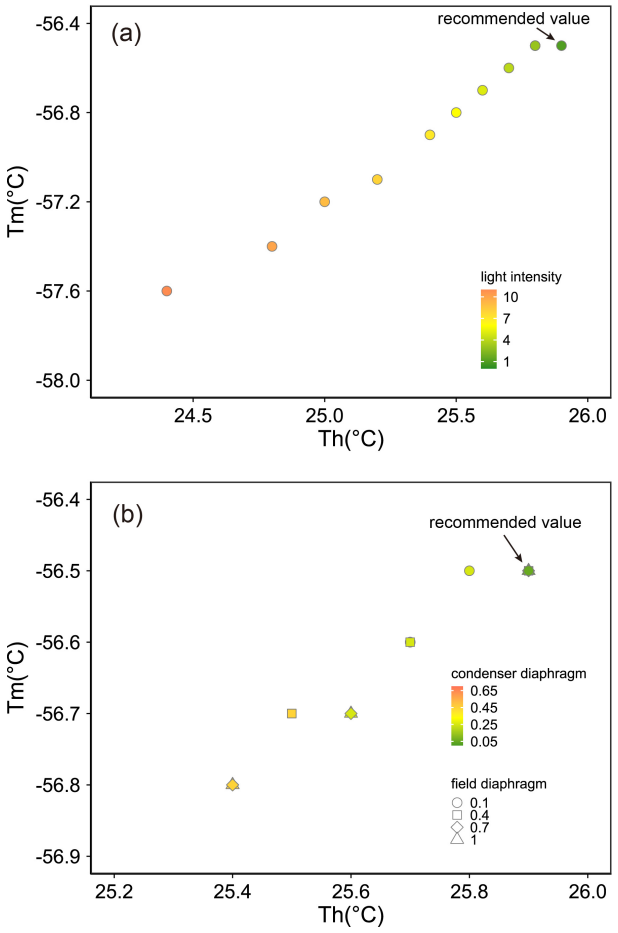

Fig. 4. Effects from infrared light intensity (a) and condenser and field diaphragms (b) on the temperature deviations during infrared microthermometry on the standard quartz-hosted CO_2 inclusion (USGS). (a): The colors inside the symbols represent different light intensities used during microthermometry. The light intensity number is proportional to the light powder but not real powder value in watt. (b): The colors inside the symbols represent different condenser diaphragms whereas symbol styles represent different field diaphragms. The light intensity of Degree 6 is used during these measurements.

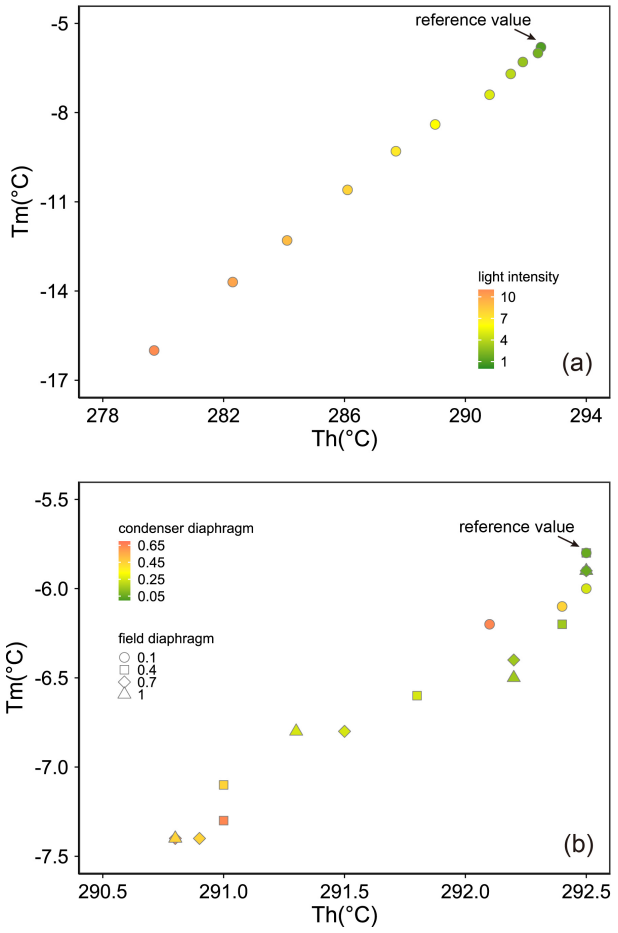

Fig. 5. Effects from infrared light intensity (a) and condenser and field diaphragms (b) on the temperature deviations during infrared microthermometry on a sphalerite-hosted saline inclusion. (a): The colors inside the symbols represent different light intensities used during microthermometry. The light intensity number is proportional to the light powder but not real powder value. (b): The colors inside the symbols represent different condenser diaphragms whereas symbol styles represent different field diaphragms. The light intensity of Degree 5 is used during these measurements.

from –28.1 °C to –20.1 °C, indicating the inclusion solute was dominated by NaCl with minor dissolved Ca^{2+}, Mg^{2+} and K^+. The final ice melting temperatures of the inclusions were in two groups. The major group was higher than –6.6 °C, while the minor group had lower values ranging from –15.7 °C to –11.1 °C. Based on the equation describing the degree of temperature depression with salinity provided by Bodnar[50], they corresponded to salinity of 1.0 to 10 wt. % and 15.1 to 19.2 wt. % NaCl equivalent, respectively (Fig. 6). The low- and high-salinity groups had differences in distribution, with the former showing a slightly higher abundance in the core of sphalerite crystals than in the rim, and the latter having an inverse pattern. In the overlapping areas, inclusions with high salinity occurred along trails that cut through the trails of low-salinity inclusions (Fig. 3f), implying a late-stage origin for the high-salinity group of fluid inclusions. During heating, the transmittance of sphalerite decreased significantly at ~200 °C, but in most cases the mineral remained observable under infrared light. Moreover, after ~5 min unremitting irradiation, the transmittance increased to a value even higher than that under room conditions. The reasons for these changes require more detailed compositional, structural and spectroscopic studies, which are beyond the scope of the present study. Fortunately, the sphalerite remained transparent when the studied inclusions homogenized. All the inclusions homogenized to liquid via bubble disappearance at temperatures ranging from 192 °C to 338 °C with the majority being at ~250–300 °C.

6 Discussion

6.1 Recommended procedure for infrared microthermometry

It has been demonstrated that infrared light can cause significant negative temperature deviations in microthermometric results, which may result in overestimation of salinity and underestimation of the T_h of fluid inclusions[44, 45]. This deviation is essentially due to the temperature discrepancies between the inclusion interior and the thermocouples mounted inside

DOI: 10.52396/JUSTC-2023-0054
JUSTC, **2024**, 54(5): 0502

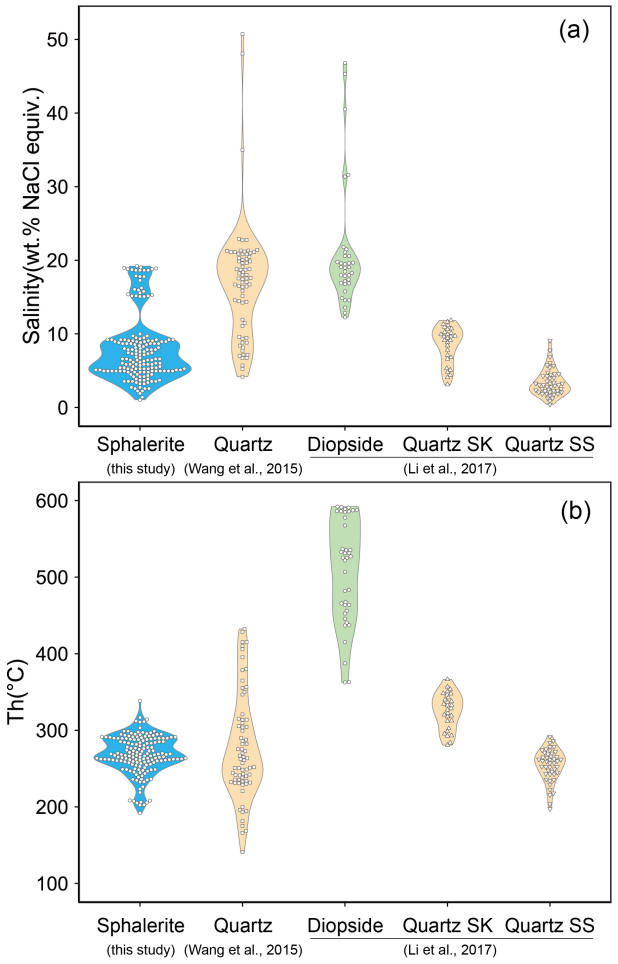

Fig. 6. Violin statistics diagrams for salinity (a) and homogenization temperature (b) of inclusions in different host minerals from the Xinqiao deposit. Data of sphalerite-hosted inclusions are from this study, where the other data sources are listed in the abscissa labels. Quartz SK: quartz in skarn. Quartz SS: quartz in sand stone.

the microthermometry stage. The higher temperature in the inclusion interior was attributed to the absorption of infrared light energy. The test measurements indicated that the temperature deviations were controlled by light intensity and the combined effects of the mineral species and inclusion type. Although a higher light intensity generally results in larger temperature deviation, the relationship between light intensity and temperature deviation is not linear and cannot be precisely predicted by any equation. Under the same light conditions, the temperature deviation for the T_m of an inclusion was comparable to that for T_h, indicating that the deviations may be an essential feature of the mineral and/or the inclusion. In addition, quartz-hosted CO_2 inclusion showed smaller temperature deviations than sphalerite-hosted saline inclusion (Figs. 6 and 7), which may be due to the limited absorption by quartz considering its large band gap energy, although the possible effect of the inclusion type cannot be precluded. In this study, the large deviations for the sphalerite-hosted saline inclusions were in significant contrast to previous observations that showed limited deviation for sphalerite-hosted saline inclusions even when light intensity was very high[44]. This may indicate that infrared light intensity-induced temperature deviations during microthermometry are related to mineral composition, as revealed by Peng et al.[45]. Even different endmembers of a solid solution series can result in discrepant temperature deviations. Therefore, the arbitrary application of previous observations or conclusions regarding the temperature deviations of fluid inclusions in minerals may give rise to incorrect results, which means that systematic test measurements must be performed before any microthermometric measurements of the mineral or of the type of inclusion.

Infrared light intensity is the key factor controlling temperature deviations during microthermometry for a particular mineral and inclusion type. All efforts, including decreasing the field and condenser diaphragms and inserting an optical filter, were made to decrease the intensity of the light irradiating the samples. Therefore, the use of the lowest possible light intensity is highly recommended during infrared microthermometry. Although decreasing the field and condenser diaphragms can help reduce possible temperature deviations, they are not recommended because very small diaphragms will probably bedim the phase boundaries of inclusions and increase the difficulty of recognizing possible phase changes. An optical filter is another recommended device, especially when test measurements showed that the lowest light intensity of the microscope was insufficient for eliminating temperature deviations. During application, the filter must match the band gap energy of the target mineral to ensure observability.

The above procedures, including test measurements, using as low as possible light intensity and inserting an optical filter, generally provide an accurate microthermometric result. However, the cycling microthermometry method (Figs. 2 and 3) is required to achieve double insurance. In most cases, the cycling microthermometry method can be used for random inspections, which may significantly reduce the measurement tasks.

6.2 Different fluids recorded by quartz and sphalerite in the Xinqiao deposit

Aqueous inclusions were the only inclusions observed in sphalerite from the Xinqiao deposit, which was consistent with the records in quartz and diopside [25, 29]. However, hypersaline inclusions with halite daughter minerals were found in gangue minerals but were absent in sphalerite. Quartz-hosted inclusions were reported to have T_h ranging from ~140 °C to ~432 °C, recording fluid mixing between high-temperature magmatic fluid and low-temperature meteoric water and fluid boiling at ~250 °C [25, 29]. By contrast, homogenization temperatures of sphalerite-hosted inclusions were more concentrated at ~250 to ~300 °C (Fig. 6), probably representing crystallization temperature for sphalerite. Although the inclusion salinity was distributed in two separate groups, seemingly conforming to fluid boiling as was recorded by quartz[25], they cannot result from fluid boiling, as the contemporaneous inclusion assemblage has similar salinity. Furthermore, fluid boiling generally results in two types of inclusions with different degrees of vapor filling. After continuous heating, they will homogenize to vapor and liquid phases, respectively[51]. This is the opposite of the inclusions studied as they all homogenized to the liquid phase. Therefore, the contrasting

DOI: 10.52396/JUSTC-2023-0054
JUSTC, **2024**, 54(5): 0502

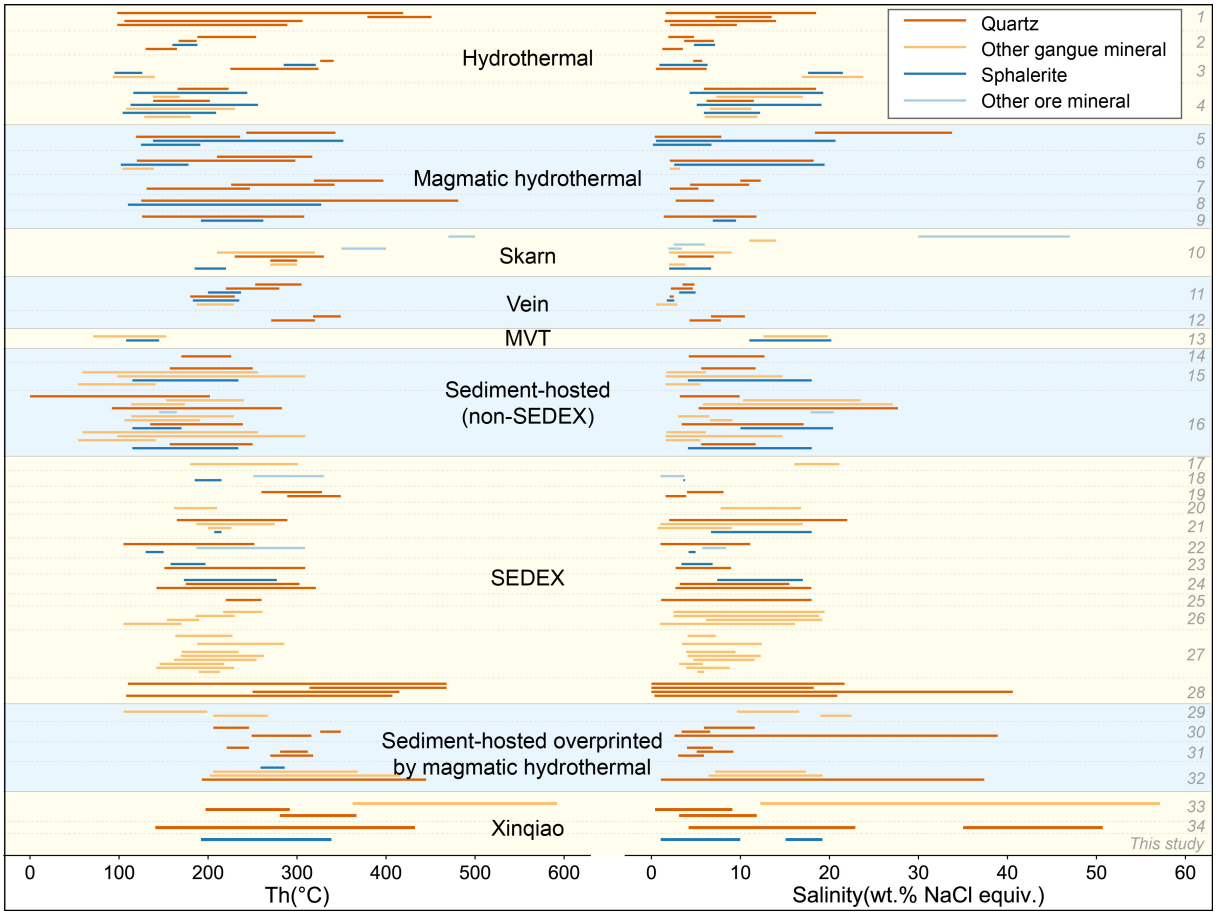

Fig. 7. Fluid inclusion microthermometric data of global sphalerite-bearing deposits. Every colorful line represents data of a particular inclusion series that are hosted in the same mineral type or formed during the same stage. The left and right endpoints of the colorful lines are minimum and maximum values (homogenization temperature and salinity) for the particular inclusion series. The alternative color regions between solid horizontal lines represent different deposit types, whereas the region between dashed horizontal line represents the individual deposit as is numbered in the right boundary. The data source could be referred in supplementary Table. MVT: Mississippi valley type. SEDEX: sedimentary exhalative deposit.

salinities of the sphalerite-hosted inclusions likely represent two independent fluids with different sources and/or evolutionary paths.

Fluid inclusion data from global sphalerite-bearing deposits show that fluid inclusions in sphalerite and quartz differ [18,33,52–55]. Depending on the metallogenic mechanism, fluid inclusions in quartz can record fluid evolution ranges from >500 °C to room temperature with salinity from 0 to >50 wt.%. By contrast, sphalerite-hosted fluid inclusions generally had temperatures of 100-400 °C with salinity ranging from ~0 to <20 wt. % (Fig. 7). Hence, sphalerite-hosted fluid inclusions may provide more precise constraints on ore-forming fluids related to sphalerite formation. In addition, global sphalerite-bearing deposits always involve high-temperature and high-salinity fluids when the sphalerite is associated with a magmatic-hydrothermal process, whereas sphalerite in sediment-hosted deposits is generally crystallized from medium-low temperature and low salinity fluids (Fig. 7). In particular, ore-forming fluids in sedimentary exhalative (SEDEX) deposits exhibited higher temperatures than those in non-SEDEX sediment-hosted deposits. For the sphalerite-hosted fluid inclusions in the Xinqiao deposit, the low-salinity group resembled those in the SEDEX deposit in terms of both salinity and temperature signatures. In contrast, the high-salinity group had a slightly higher temperature and salinity than those in the normal sediment-hosted mineralization group, showing a closer affinity with magmatic-hydrothermal fluids. Consequently, the fluid inclusions in the Xinqiao deposit likely record a complex ore-forming fluid evolution involving SEDEX mineralization and magmatic-hydrothermal circulation. This interpretation is consistent with the distribution characteristics and relative age of the two groups of fluid inclusions (Fig. 3f) which implies that the high-salinity group (probably representing magmatic-hydrothermal fluids) was superimposed on the low-salinity inclusions (representing SEDEX fluids). This was further verified by the highly similar fluid inclusion data in gangue minerals from the Xinqiao deposit with those from deposits such as the Anjing Hitam Pb-Zn deposit in Indonesia[56] and the Talate Pb-Zn deposit in Xinjiang province[57], which were all first mineralized during the sedimentation process and then overprinted by late-stage magmatic-hydrothermal fluids.

6.3 Implications for the metallogenic mechanism of the Xinqiao deposit

Previous fluid inclusion studies on the Xinqiao deposit sug-

DOI: 10.52396/JUSTC-2023-0054
JUSTC, **2024**, 54(5): 0502

gested a carbonate replacement genesis associated with the Yanshanian Jitou monzodiorite[29]. However, the sphalerite-hosted inclusions in this study demonstrate that SEDEX-related fluids played a significant role. The SEDEX-related metallogenic event has been verified by sulfide Re-Os isotopic dating[23, 25], pyrite composition[26, 58, 59] and tectonic evidence[60]. Additionally, such a metallogenic event is frequently reported with respect to other deposits in the Tongling mineralization district[58, 61–63], further demonstrating the significant role of sedimentary exhalation in regional mineralization.

As fluid inclusion data for other sulfides are lacking, fluid inclusions in gangue minerals are still the best proxy for metallogenic fluids in the magmatic-hydrothermal stage of the Xinqiao deposit. After compiling all the published fluid inclusion data, a clear four-stage fluid evolution was observed (Fig. 8). Stage I was characterized by low-salinity fluid inclusions hosted in the sphalerite. This record was highly consistent with ore-forming fluid signatures in the SEDEX deposits which generally involved seawater (low salinity) as the ultimate fluid source[54, 64]. Moreover, fluid inclusions in quartz vein hosted in sandstone showed similar temperature and salinity signatures[29], and could be regarded as a supplementary record for SEDEX-related fluids. The fluid inclusions in Stage II had high temperatures and salinities. The inclusions were mainly hosted in diopside and a small section of quartz in the Jitou monzodiorite, likely representing an early stage of magmatic fluid [25, 29]. Stage III was probably the main stage of magmatic hydrothermal mineralization. Fluid inclusions during this stage were of medium temperature, from ~220 to 380 °C, but with complex salinity records. The fluid boiling process in this temperature range was clearly demonstrated in a previous study[25], particularly based on inclusion pairs with similar homogenization temperatures but contrasting salinities and different homogenization modes during microthermometry. The fluid inclusions in the banded quartz vein from skarn ore were reported to have similar temperature (~–280 to 380 °C) but low salinity (~3–12 wt. %)[29]. Although the homogenization modes for the inclusions have not been reported[29], at least some of them could be inferred to have homogenized to the vapor phase based on the reported high filling degree of the vapor (as high as 50%). Hence, they represent the low-salinity group after fluid boiling process. Wang et al.[25] found that the high-salinity group from the fluid boiling process was characterized by quartz-hosted inclusions. Additionally, in this study, the high-salinity inclusions hosted in the sphalerite had similar signatures, probably recording trails associated with fluid boiling. Because the fluid boiling process was restricted to magmatic hydrothermal circulation and because the sphalerite in this study was collected from bedded ore bodies, the high-salinity fluids in some crystals indicated a certain degree of modification of the SEDEX ore bodies by magmatic hydrothermal fluids. Stage IV fluid inclusions had low temperatures and low salinities, representing meteoric water after the major metallogenic stage. In addition, from Stage II to Stage IV, i.e., the entire magmatic-hydrothermal fluid evolution, the salinity decreased with decreasing temperature, indicating fluid mixing between the magmatic fluid and meteoric water[25].

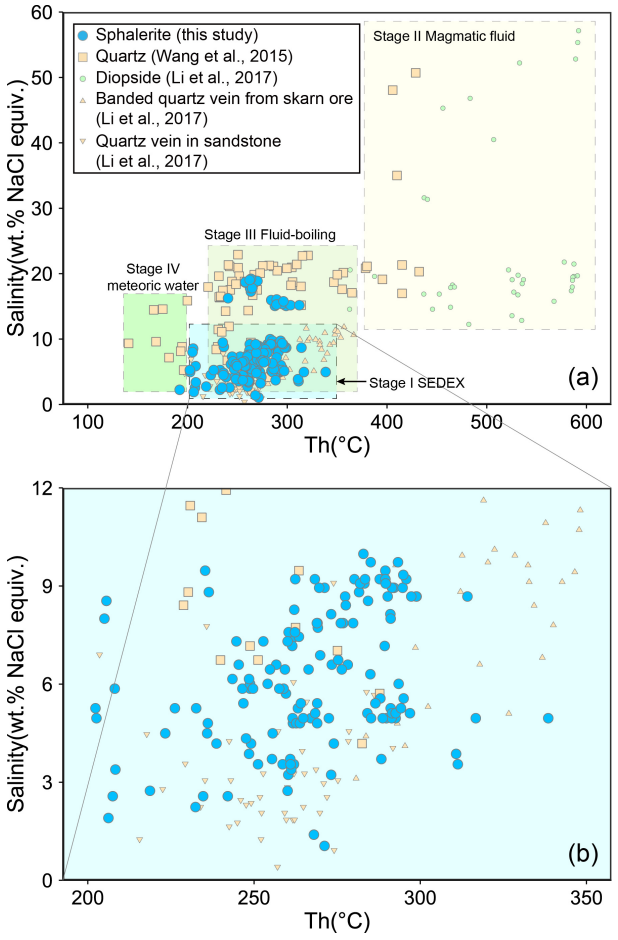

Fig. 8. Salinity versus homogenization temperature diagram of the inclusions in the Xinqiao deposit. The four-stage ore-forming fluid evolution is illustrated as four different dashed boxes. Panel b is the amplifying diagram of the data in Stage I box. SEDEX: sedimentary exhalative deposit.

The above four-stage ore-forming fluid evolution indicates that fluid-boiling and magmatic-meteoric water mixing played a significant role in the magmatic-hydrothermal metallogenic stage (skarn-type). Furthermore, fluid inclusions in the sphalerite confirm that the Xinqiao deposit was formed by early SEDEX mineralization and then replaced by later magmatic-hydrothermal fluids.

7 Conclusions

Infrared light can cause non-negligible deviations in the temperature measured during microthermometry. Our test measurements indicate that the lowest light intensity is highly recommended for infrared microthermometry. Compared with decreasing the field and condenser diaphragms, an optical filter is more effective, especially when test measurements show that the lowest light intensity of the microscope is insufficient to eliminate temperature deviations. In addition, considering that the extent of deviation differs depending on the host mineral and fluid inclusion type, before employing infrared microthermometry, systematic test measurements are indispensable in depicting the ore-forming fluid evolution for a target geological process.

The fluid inclusions hosted in sphalerite collected from

DOI: 10.52396/JUSTC-2023-0054
JUSTC, **2024**, 54(5): 0502

bedded ore bodies in the Xinqiao deposit were aqueous without CO_2. They show homogenization temperature of ~200–350 °C, but with two separated salinity groups, probably representing two separated fluids unrelated to fluid boiling. Bulk fluid inclusions were highly similar to those of deposits that involved a combination of SEDEX and magmatic hydrothermal mineralization. In summary, a four-stage fluid evolution can be depicted, including (I) medium-temperature and low-salinity SEDEX-associated fluid (fluid inclusions hosted in sphalerite), (II) high-temperature and high-salinity magmatic fluid (fluid inclusions hosted in diopside and quartz), (III) medium-temperature and medium-salinity magmatic fluid with a fluid boiling process (fluid inclusions hosted in quartz and sphalerite), and (IV) low-temperature and low-salinity meteoric water (fluid inclusions hosted in quartz). Fluid mixing between the magmatic fluid and meteoric water probably played a role during Stages II–IV. The fluid evolution confirmed that the Xinqiao deposit was formed by two-stage metallogenic events including SEDEX and magmatic-hydrothermal mineralization.

Supporting information

The supporting information for this article can be found online at http://doi.org/10.52396/JUST-2023-0054. It includes one table.

Acknowledgements

This work was supported by the Fundamental Research Funds for the Central Universities (WK3410000015).

Conflict of interest

The authors declare that they have no conflict of interest.

Biographies

Yangyang Wang is an Associate Research Fellow at the School of Earth and Space Sciences, University of Science and Technology of China (USTC). He received his Ph.D. degree from the USTC in 2017. His research mainly focuses on fluid inclusion and isotope geochemistry.

Yilin Xiao is a Professor at the School of Earth and Space Sciences, University of Science and Technology of China. He received his Ph.D. degree from the University of Goettingen (Germany) in 2001. His research mainly focuses on geological fluids, metamorphism in subduction zones, trace element and isotope geochemistry.

References

[1] Campbell A R, Robinsoncook S. Infrared fluid inclusion microthermometry on coexisting wolframite and quartz. *Economic Geology*, **1987**, *82* (6): 1640–1645.

[2] Campbell A R, Panter K S. Comparison of fluid inclusions in coexisting (cogenetic?) wolframite, cassiterite, and quartz from St. Michael's Mount and Cligga Head, Cornwall, England. *Geochimica et Cosmochimica Acta*, **1990**, *54* (3): 673–681.

[3] Lüders V. Contribution of infrared microscopy to fluid inclusion studies in some opaque minerals (wolframite, stibnite, bournonite): Metallogenic implications. *Economic Geology and the Bulletin of the Society of Economic Geologists*, **1996**, *91* (8): 1462–1468.

[4] Wilkinson J J, Stoffell B, Wilkinson C C, et al. Anomalously metal-rich fluids form hydrothermal ore deposits. *Science*, **2009**, *323* (5915): 764–767.

[5] Kouzmanov K, Pettke T, Heinrich C A. Direct analysis of ore-precipitating fluids: Combined IR microscopy and LA-ICP-MS study of fluid inclusions in opaque ore minerals. *Economic Geology*, **2010**, *105* (2): 351–373.

[6] Wei W F, Hu R Z, Bi X W, et al. Infrared microthermometric and stable isotopic study of fluid inclusions in wolframite at the Xihuashan tungsten deposit, Jiangxi Province, China. *Mineralium Deposita*, **2012**, *47* (6): 589–605.

[7] Krolop P, Burisch M, Richter L, et al. Antimoniferous vein-type mineralization of the Berga Antiform, Eastern-Thuringia, Germany: A fluid inclusion study. *Chemical Geology*, **2019**, *508*: 47–61.

[8] Naglik B, Dumanska-Slowik M, Tobola T, et al. Diversity of pyrite-hosted solid inclusions and their metallogenic implications: A case study from the Myszkow Mo–Cu–W porphyry deposit (the Krakow-Lubliniec Fault Zone, Poland). *Minerals*, **2021**, *11* (12): 1426.

[9] Sośnicka M, de Graaf S, Morteani G, et al. The Schlaining quartz-stibnite deposit, Eastern Alps, Austria: constraints from conventional and infrared microthermometry and isotope and crush-leach analyses of fluid inclusions. *Mineralium Deposita*, **2022**, *57* (5): 725–741.

[10] Ni P, Li W S, Pan J Y, et al. Fluid processes of wolframite-quartz vein systems: Progresses and challenges. *Minerals*, **2022**, *12* (2): 237.

[11] Bailly L, Bouchot V, Beny C, et al. Fluid inclusion study of stibnite using infrared microscopy: An example from the Brouzils antimony deposit (Vendee, Armorican Massif, France). *Economic Geology and the Bulletin of the Society of Economic Geologists*, **2000**, *95* (1): 221–226.

[12] Bailly L, Grancea L, Kouzmanov K. Infrared microthermometry and chemistry of wolframite from the Baia Sprie epithermal deposit, Romania. *Economic Geology and the Bulletin of the Society of Economic Geologists*, **2002**, *97* (2): 415–423.

[13] Shimizu T, Morishita Y. Petrography, chemistry, and near-infrared microthermometry of indium-bearing sphalerite from the Toyoha polymetallic deposit, Japan. *Economic Geology*, **2012**, *107* (4): 723–735.

[14] Lüders V. Contribution of infrared microscopy to studies of fluid inclusions hosted in some opaque ore minerals: possibilities, limitations, and perspectives. *Mineralium Deposita*, **2017**, *52* (5): 663–673.

[15] Ni P, Wang X D, Wang G G, et al. An infrared microthermometric study of fluid inclusions in coexisting quartz and wolframite from Late Mesozoic tungsten deposits in the Gannan metallogenic belt, South China. *Ore Geology Reviews*, **2015**, *65*: 1062–1077.

[16] Ni P, Li W S, Pan J Y. Ore-forming fluid and metallogenic mechanism of wolframite-quartz vein-type tungsten deposits in South China. *Acta Geologica Sinica (English Edition)*, **2020**, *94* (6): 1774–1796.

[17] Ortelli M, Kouzmanov K, Wälle M, et al. Fluid inclusion studies in opaque ore minerals: I. Trace element content and physical properties of ore minerals controlling textural features in transmitted near-infrared light microscopy. *Economic Geology*, **2018**, *113* (8): 1845–1860.

[18] Korges M, Weis P, Luders V, et al. Sequential evolution of Sn–Zn–In mineralization at the skarn-hosted Hammerlein deposit, Erzgebirge, Germany, from fluid inclusions in ore and gangue minerals. *Mineralium Deposita*, **2020**, *55* (5): 937–952.

[19] Mao J W, Xie G Q, Duan C, et al. A tectono-genetic model for porphyry–skarn–stratabound Cu–Au–Mo–Fe and magnetite–apatite deposits along the Middle–Lower Yangtze River Valley, Eastern China. *Ore Geology Reviews*, **2011**, *43* (1): 294–314.

[20] Zhou T F, Fan Y, Yuan F, et al. Progress of geological study in the Middle–Lower Yangtze River Valley metallogenic belt. *Acta Petrologica Sinica*, **2012**, *28* (10): 3051–3066. (in Chinese)

[21] Zhou T F, Fan Y, Wang S W, et al. Metallogenic regularity and

DOI: 10.52396/JUSTC-2023-0054
JUSTC, **2024**, 54(5): 0502

metallogenic model of the Middle–Lower Yangtze River Valley metallogenic belt. *Acta Petrologica Sinica*, **2017**, *33* (11): 3353–3372. (in Chinese)

[22] Gu L, Khin Z, Hu W, et al. Distinctive features of Late Palaeozoic massive sulphide deposits in South China. *Ore Geology Reviews*, **2007**, *31*: 107–138.

[23] Guo W M, Lu J J, Jiang S Y, et al. Re-Os isotope dating of pyrite from the footwall mineralization zone of the Xinqiao deposit, Tongling, Anhui Province: Geochronological evidence for submarine exhalative sedimentation. *Chinese Science Bulletin*, **2011**, *56* (35): 3860–3865.

[24] Xie J C, Yang X Y, Sun W D, et al. Geochronological and geochemical constraints on formation of the Tongling metal deposits, middle Yangtze metallogenic belt, east-central China. *International Geology Review*, **2009**, *51* (5): 388–421.

[25] Wang Y Y, Xiao Y L, Yang X Y. Re-Os isotope systematics and fluid inclusions of Xinqiao deposit in Tongling, the Middle–Lower Yangtze River Metallogenic Belt. *Acta Petrologica Sinica*, **2015**, *31* (4): 1031–1039. (in Chinese)

[26] Xiao X, Zhou T F, Fan Y, et al. LA-ICP-MS in situ trace elements and FE-SEM analysis of pyrite from the Xinqiao Cu–Au–S deposit in Tongling, Anhui and its constraints on the ore genesis. *Acta Petrologica Sinica*, **2016**, *32* (2): 369–376. (in Chinese)

[27] Zhang Y, Shao Y J, Li H B, et al. Genesis of the Xinqiao Cu–S–Fe–Au deposit in the Middle–Lower Yangtze River Valley metallogenic belt, Eastern China: Constraints from U–Pb–Hf, Rb–Sr, S, and Pb isotopes. *Ore Geology Reviews*, **2017**, *86*: 100–116.

[28] Zhang Y, Shao Y J, Wu C D, et al. LA-ICP-MS trace element geochemistry of garnets: Constraints on hydrothermal fluid evolution and genesis of the Xinqiao Cu–S–Fe–Au deposit, Eastern China. *Ore Geology Reviews*, **2017**, *86*: 426–439.

[29] Li Y, Li J W, Li X H, et al. An Early Cretaceous carbonate replacement origin for the Xinqiao stratabound massive sulfide deposit, Middle–Lower Yangtze Metallogenic Belt, China. *Ore Geology Reviews*, **2017**, *80*: 985–1003.

[30] Shuey R T. Semiconducting Ore Minerals. New York: Elsevier, **1975**.

[31] Boldish S I, White W B. Optical band gaps of selected ternary sulfide minerals. *American Mineralogist*, **1998**, *83*: 865–871.

[32] Ni P, Zhu X, Wang R, et al. Constraining ultrahigh-pressure (UHP) metamorphism and titanium ore formation from an infrared microthermometric study of fluid inclusions in rutile from Donghai UHP eclogites, eastern China. *GSA Bulletin*, **2008**, *120*: 1296–1304.

[33] Bauer M E, Burisch M, Ostendorf J, et al. Trace element geochemistry of sphalerite in contrasting hydrothermal fluid systems of the Freiberg district, Germany: insights from LA-ICP-MS analysis, near-infrared light microthermometry of sphalerite-hosted fluid inclusions, and sulfur isotope geochemistry. *Mineralium Deposita*, **2019**, *54*: 237–262.

[34] Peng H W, Fan H R, Lecumberri-Sanchez P, et al. Fluid evolution and ore genesis of the Tiantangshan granite-related vein-type Rb–Sn–W deposit, south China: constraints from LA-ICP-MS analyses of fluid inclusions. *Mineralium Deposita*, **2023**, *58* (4): 751–769.

[35] Lindaas S E, Kulis J, Campbell A R. Near-infrared observation and microthermometry of pyrite-hosted fluid inclusions. *Economic Geology*, **2002**, *97* (3): 603–618.

[36] Pflugbeil B. Mikrothermometrische Untersuchungen an Flüssigkeitseinschlüssen in Wolframiten aus Quarz-Wolframit-Mineralisationen mittels IR-Mikroskopie. Thesis. Berlin: Technische Universität Berlin, **1995**: 59.

[37] Shimizu T, Aoki M, Kabashima T. Near-infrared and visible light microthermometry of fluid inclusions in sphalerite from a possible southeast extension of the Toyoha polymetallic deposit, Japan. *Resource Geology*, **2003**, *53* (2): 115–126.

[38] Rosiere C A, Rios F J. The origin of hematite in high-grade iron ores based on infrared microscopy and fluid inclusion studies: The example of the Conceicao Mine, Quadrilatero Ferrifero, Brazil. *Economic Geology and the Bulletin of the Society of Economic Geologists*, **2004**, *99* (3): 611–624.

[39] Lüders V, Ziemann M. Possibilities and limits of infrared light microthermometry applied to studies of pyrite-hosted fluid inclusions. *Chemical Geology*, **1999**, *154*: 169–178.

[40] Kouzmanov K, Bailly L, Ramboz C, et al. Morphology, origin and infrared microthermometry of fluid inclusions in pyrite from the Radka epithermal copper deposit, Srednogorie zone, Bulgaria. *Mineralium Deposita*, **2002**, *37* (6-7): 599–613.

[41] Zhu M T, Zhang L C, Wu G, et al. Fluid inclusions and He–Ar isotopes in pyrite from the Yinjiagou deposit in the southern margin of the North China Craton: A mantle connection for poly-metallic mineralization. *Chemical Geology*, **2013**, *351*: 1–14.

[42] Moritz R. Fluid salinities obtained by infrared microthermometry of opaque minerals: Implications for ore deposit modeling — A note of caution. *Journal of Geochemical Exploration*, **2006**, *89*: 284–287.

[43] Ge X, Su W C, Zhu L Y, et al. A study on the influence of infrared light source intensity on salinity of fluid inclusion in opaque mineral by using infrared microthermometry: in the case of stibnite. *Acta Mineralogica Sinica*, **2011**, *31*: 366–371. (in Chinese)

[44] Casanova V, Kouzmanov K, Audetat A, et al. Fluid inclusion studies in opaque ore minerals: II. A comparative study of syngenetic synthetic fluid inclusions hosted in quartz and opaque minerals. *Economic Geology*, **2018**, *113* (8): 1861–1883.

[45] Peng H W, Fan H R, Santosh M, et al. Infrared microthermometry of fluid inclusions in transparent to opaque minerals: challenges and new insights. *Mineralium Deposita*, **2020**, *55* (7): 1425–1440.

[46] Goldstein R H, Reynolds T J. Systematics of Fluid Inclusions in Diagenetic Minerals. Tulsa, USA: SEPM (Society for Sedimentary Geology), **1994**.

[47] Zhu X, Ni P, Huang J B, et al. Introduction to Infrared micro-thermometric technique: An example from fluid inclusion study in rutile deposits. *Acta Petrologica Sinica*, **2007**, *23* (9): 2052–2058.

[48] Li Y S, Zhang B L, Gong F Y, et al. Genesis of the giant Kangjiawan lead-zinc ore deposit in Hunan Province: Evidences from fluid inclusion, H-O and S isotope. *Acta Petrologica Sinica*, **2021**, *37* (6): 1847–1866.

[49] Wang Y B, Liu D Y, Meng Y F, et al. SHRIMP U-Pb geochronology of the Xinqiao Cu-S-Fe-Au deposit in the Tongling ore district, Anhui. *Chinese Geology*, **2004**, *31* (2): 169–173.

[50] Bodnar R J. Revised equation and table for determining the freezing-point depression of H2O-NaCl solutions. *Geochimica et Cosmochimica Acta*, **1993**, *57* (3): 683–684.

[51] Ramboz C, Pichavant M, Weisbrod A. Fluid immiscibility in natural processes: Use and misuse of fluid inclusion data. 2. Interpretation of fluid inclusion data in terms of immiscibility. *Chemical Geology*, **1982**, *37* (1-2): 29–48.

[52] Wang D, Zheng Y, Yang W, et al. Geology, mineralogy, fluid inclusion, and H–O–S–Pb isotope constraints on ore genesis of the Keyue Sb–Pb–Zn–Ag deposit in Southern Tibet. *Geofluids, 2018*, **2018**3175423.

[53] Wang Z G, Wang K Y, Wan D, et al. Genesis of the Huanggoushan Pb–Zn–Au polymetallic deposit in southern Jilin Province, NE China: Constraints from fluid inclusions and C–H–O–S–Pb isotope systematics. *Geological Journal*, **2020**, *55* (4): 3112–3138.

[54] Hanilçi N, Öztürk H, Banks D, et al. Geological, geochemical and microthermometric characteristics of the Hakkari region Zn-Pb deposits, SE Turkey. *Ore Geology Reviews*, **2020**, *125*: 103667.

[55] Siani M G, Mehrabi B, Nazarian M, et al. Geology and genesis of the Chomalu polymetallic deposit, NW Iran. *Ore Geology Reviews*, **2022**, *143*: 104763.

[56] Huang C, Du G, Jiang H, et al. Ore-forming fluids characteristics and metallogenesis of the Anjing Hitam Pb-Zn deposit in Northern Sumatra, Indonesia. *Journal of Earth Science*, **2019**, *30* (1):

DOI: 10.52396/JUSTC-2023-0054
JUSTC, **2024**, 54(5): 0502

131–141.
[57] Yang J, Yang X, Yang C, et al. Genesis of the Talate Pb–Zn (–Fe) deposit in the Altay, Xinjiang, NW China: Evidence from fluid inclusions and stable isotopes. *Ore Geology Reviews*, **2022**, *144*: 104864.
[58] Xu J, Xie Y, Yang Z, et al. Trace elements in fluid inclusions of submarine exhalation-sedimentation system in Tongling metallogenic province. *Mineral Deposits*, **2004**, *23* (3): 344–352.
[59] Zhou T F, Zhang L J, Yuan F, et al. LA-ICP-MS in situ trace element analysis of pyrite from the Xinqiao Cu–Au–S deposit in Tongling, Anhui, and its constraints on the ore genesis. *Earth Science Frontiers*, **2010**, *17* (2): 306–319. (in Chinese)
[60] Xu G, Zhou J. The Xinqiao Cu–S–Fe–Au deposit in the Tongling mineral district, China: synorogenic remobilization of a stratiform sulfide deposit. *Ore Geology Reviews*, **2001**, *18*: 77–94.
[61] Xiao X, Gu L, Ni P, et al. Study on fluids of SEDEX massive sulfide deposits in Tongling district, Anhui Province. *Mineral Deposits*, **2002**, *21* (Suppl.): 491–494. (in Chinese)
[62] Xu W Y, Yang Z S, Meng Y F, et al. Genetic model and dynamic migration of ore-forming fluids in carboniferous exhalation-sedimentary massive sulfide deposits of Tongling district, Anhui Province. *Mineral Deposits*, **2004**, *23* (3): 353–364.
[63] Jiang S Y, Ding Q F, Yang S Y, et al. Discovery and significance of carbonate mud mounds from Cu-polymetallic deposits in the middle and Lower Yangtze Metallogenic Belt: Examples from the Wushan and Dongguashan deposits. *Acta Geologica Sinica*, **2011**, *85* (5): 744–756. (in Chinese)
[64] Mahmoodi P, Rastad E, Rajabi A, et al. Genetic model for Jurassic shale-hosted Zn-Pb deposits of the Arak Mining District, Malayer-Esfahan metallogenic belt: Insight from sedimentological, textural, and stable isotope characteristics. *Ore Geology Reviews*, **2021**, *136*: 104262.

DOI: 10.52396/JUSTC-2023-0054
JUSTC, **2024**, 54(5): 0502